Local models for artefact reduction in iterative CT reconstruction

Katrien Van Slambrouck and Johan Nuyts

Abstract—**Metal artefact reduction (MAR) in computed tomography remains a challenging problem. Projection completion (PC) and iterative reconstruction with an advanced projection model are the two most important MAR methods. PC often results in strong artefact reduction, but by the interpolation step information about the metal and its surrounding is lost. This information can be important in e.g. orthopaedic surgery for implant follow-up. Iterative methods use all available information and are more suitable in such cases. Unfortunately, these methods are slow, especially when using a more adequate, more complex model. We present a local model reconstruction scheme which uses iterative reconstruction but only increases the complexity of the model in the vicinity of metals. Hereby we can limit the computation time while keeping a similar image quality. Moreover, when using a sequential update of several image parts, one obtains a better convergence of the metals, leading to an improved artefact reduction.**

I. Introduction

Computed tomography (CT) reconstruction often suffers from severe artefacts when there are highly attenuating objects (such as metals) present in the scanned object. Metal artefact reduction methods can be divided into two main groups: projection completion based methods and methods based on iterative reconstruction with an advanced model. Projection completion (PC) is based on the idea that metal projections are corrupted. The metal projections are thus removed form the measurement and replaced by interpolated projections. Different interpolation methods exist (e.g. linear [1], polynomial [2], [3], ... interpolation). Mostly PC is based on FBP (filtered backprojection) reconstruction, which makes it a fast method. The disadvantage of these methods is the loss of information when removing the projection data, in first instance the shape and attenuation of the metal itself. The metal shape and attenuation values in the final reconstruction are totally based on the initial reconstruction made to select the metals. Moreover, also information about structures close to metals or in between metals is (partly) lost. This can lead to new artefacts or deformation of structures lying in the projection rays that are removed and interpolated, in particular structures close to the metals. PC is not ideal for application where one is interested in these regions as for example in implant follow-up in orthopaedic surgery.

Iterative methods use all measured information, thus also about the metals and their surroundings (as long as there is no full photon starvation). Metal artefacts are reduced by the use of a more adequate model. In case of metal artefacts the model includes e.g. the polychromatic nature of the x-ray beam emerging form the tube. (A more extended overview of metal artefacts and their causes can be found in [4] and [5]). For iterative methods, the main disadvantage is the computation time which can increase enormously when the acquisition models are becoming more and more complex. In this work, we show that we only have to increase the model complexity in the vicinity of metals, keeping a less complex model for the remainder of the image without losing image quality. Moreover, when applying a sequential image-block, update for the different parts of the image, one can achieve a better metal convergence leading to an improved artefact reduction.

Dept. of Nuclear Medicine, K.U.Leuven, B-3000 Leuven, Belgium. This work is supported by the SBO-project QUANTIVIAM (060819) of the Institute for the Promotion of Innovation through Science and Technology in Flanders (IWT-Vlaanderen).

II. Methods

Our local algorithm will be based on *the patchwork projector* [6]. It divides the image into different regions or patches, and defines a suitable projection model for each patch. The complexity of the model will be increased in patches containing metals. In the following, the different steps in defining the patches and their corresponding model are explained.

A. Defining the patches in the reconstruction domain

The patches are defined by a thresholding method which selects highly attenuating objects from an initial reconstruction. The accuracy of the metal delineation is not crucial because it will not define the shape of the metal in the final reconstruction, although it is desirable that the whole metal is included. Each metallic region will be a separate patch. A last patch is defined as the whole reconstruction volume without the smaller patches.

B. The reconstruction model

The reconstruction with local models is done by a maximum likelihood reconstruction algorithm based on the Poisson likelihood:

$$L = \sum_i \left(y_i \ln \hat{y}_i - \hat{y}_i \right) \tag{1}$$

with i the index of the projection lines, y_i the measured transmission scan and $\hat{y}_i$ the estimated transmission scan based on the (current) reconstruction image. The update for each of the parameters μ_j, the linear attenuation coefficient of pixel j, is calculated as in [7]:

$$\mu_j^{\text{new}} = \mu_j^{\text{old}} - \frac{\left.\frac{\partial L}{\partial \mu_j}\right|_{\vec{\mu}^{\text{old}}}}{\sum_h \left.\frac{\partial^2 L}{\partial \mu_j \partial \mu_h}\right|_{\vec{\mu}^{\text{old}}}} \tag{2}$$

For each of the patches a different projection model $\hat{y}_i$ can be chosen. The models differ in their energy and resolution properties.

1) The energy model:

a) Monochromatic model, MLTR: The monochromatic model is the one used in MLTR (maximum likelihood for transmission) [7]:

$$\hat{y}_i = b_i \exp\big(-\sum_j l_{ij}\mu_j\big) \tag{3}$$

with b_i the blank value for projection line i and l_{ij} the intersection length of projection line i and pixel j. Updating the whole image for one iteration results in 3 (back)projections.

b) Polychromatic water model, MLTRC: MLTRC is a polychromatic extension of MLTR which takes into account the polychromatic behaviour of the X-rays going through water. The projection model becomes:

$$\hat{y}_i = \sum_k b_{ik} \exp\big(-P_k \sum_j l_{ij}\mu_j\big), \quad P_k = \frac{\mu_{\mathrm{k}}^{\mathrm{water}}}{\mu_{ref}^{\mathrm{water}}} \tag{4}$$

with k the energy bin and b_{ik} the blank value for projection line i at energy k. Note that the complexity (in terms of (back)projections) of this model is the same as that of regular MLTR.

c) Full polychromatic model, IMPACT: The IMPACT (iterative maximum likelihood polychromatic algorithm for CT) [8] projection model uses a fully polychromatic projection estimate:

$$\hat{y}_i = \sum_k b_{ik} \exp\left(-\Theta_k \sum_j l_{ij}\theta(\mu_{j,\mathrm{ref}}) - \Phi_k \sum_j l_{ij}\theta(\mu_{j,\mathrm{ref}})\right). \tag{5}$$

The energy dependent linear attenuation is written as a linear combination of the Compton and photo electric component, with Θ_k and Φ_k the energy dependence of respectively Compton scattering and the photo electric effect, and θ_j and ϕ_j the material dependence. We assume that θ_j and ϕ_j are unambiguously determined by the attenuation at a chosen reference energy: $\theta_j = \theta(\mu_{j,\mathrm{ref}})$ and $\phi_j = \phi(\mu_{j,\mathrm{ref}})$. The complexity for each update is 8 (back)projections.

2) The resolution model: The resolution is modelled by subsampling the detector elements (S samples) and decreasing the pixel size in the reconstruction image ($M = J * f$, the new number of pixels with f the (integer) size factor and J the original number of pixels).

$$\hat{y}_i = \sum_s b_{is} \exp\big(-\sum_m l_{ism}\mu_m\big) \tag{6}$$

C. Updating the patches

During the reconstruction the patches are sequentially updated as a group of pixels in a grouped coordinate algorithm [9], each time using their own projection model. The combined projection estimate becomes:

$$\hat{y}_i = \sum_k b_{ik} \prod_p \exp(-\hat{z}_{ik,p}) \tag{7}$$

with p the patch index and $\hat{z}_{ik,p}$ the projection of the attenuation values for projection ray i and patch p at energy k.

D. Scatter

The influence of scatter is not always negligible. As a first order correction we add a position independent scatter term R in our model, which is updated in each iteration. The update strategy is the same as in (2). Which gives:

$$\hat{y}_i^R = \hat{y}_i + R, \quad L = \sum_i \big(y_i \ln \hat{y}_i^R - \hat{y}_i^R\big) \tag{8}$$

$$R^{\mathrm{new}} = R^{\mathrm{old}} - \frac{\frac{\partial L}{\partial R}}{\frac{\partial^2 L}{\partial R^2}}. \tag{9}$$

This is a sinogram procedure, and therefore independent of the patches.

III. Experiments

A. Phantoms and scan parameters

Two phantoms were scanned on a Siemens Sensation 16 CT (part of Biograph 16 PET/CT system), using a circular scan of 0.5 s per rotation, tube voltage 120 kV and tube current 300 mA. The phantoms were scanned with collimation 2 x 1.00 mm.

The first phantom is a circular PMMA (polymethyl methacrylate) phantom (19 cm diameter) with two aluminium inserts (3 cm diameter) and two iron inserts (1 cm diameter). The other phantom is body shaped with two hip implants (CoCr and Ti), one aluminium insert (3 cm diameter) and seven small PMMA details (1 cm diameter) around the CoCr implant.

B. Reconstruction parameters

We selected one slice for a two dimensional reconstruction with a pixel size of 0.97 mm. During reconstruction we used a distance driven projector [10].

We applied a regular FBP reconstruction and two PC methods. The first PC method is the linear interpolation method of Kalender at al. [1] (referred to as PC). The second method adds a normalization step to the procedure, still using linear interpolation [11], [12] (referred to as PC-NMAR). For segmentation of the metals we used a k-means clustering. Note that when using PC, the initial segmentation of the metals defines their shape in the final reconstruction.

For the iterative methods we applied a regular IMPACT reconstruction. This means that no patches are involved and the same energy and resolution model is used for the whole volume. In a second step we divided the image into patches, increasing the resolution ($S = 3$, $f = 3$) for the patches containing the implants. Here we apply the sequential update for the patches. Finally a different energy model was used in the different patches. The patches containing metals will be

Patched IMPACT

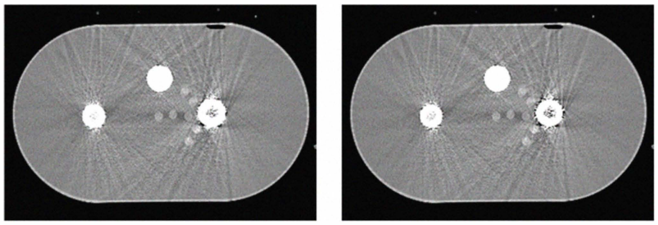

Increased resolution for implant patches | No increase of resolution for implant patches

Fig. 3. **Resolution**. Comparison of reconstruction with Patched IMPACT with and without the increased resolution for the patches with the implants. Windowed in interval [-700, 500] HU.

reconstructed with the IMPACT energy model and increased resolution for those patches that contain the implants ($S = 3$, $f = 3$). The remainder of the reconstruction volume is reconstructed with MLTRC. For all iterative methods 20 iterations with 116 subsets were used.

IV. Results

Figure 1 shows the results for the circular phantom. We see that PC yields an almost perfect reconstruction, with PC-NMAR even better. IMPACT still has some artefacts which are reduced when using the patches. The introduction of MLTRC as projection model for the non-metals parts of the images has no influence on the image quality.

For the body-shaped phantom, the results are shown in figure 2. PC methods result in less streak and shadow artefacts but the PMMA details are deformed or even almost erased. The iterative methods result in an image with more streak and shadow artefacts but the PMMA details are much better reconstructed.

To investigate the influence of the resolution model, a reconstruction with and without increased resolution for the implant patches was performed for the body phantom. The results are shown in figure 3. The obtained reconstructions are very similar.

V. Discussion

PC is often used in metal artefact reduction because it results in a clear artefact reduction in a limited time. This is shown for the reconstructions of the circular phantom. PC-NMAR with the included normalization results in an almost perfect reconstruction, where the iterative methods still show some artefacts. The reconstruction of the body phantom is different. Also here, few streak and shadow artefacts remain for the PC methods but the PMMA details are severely deformed in the reconstruction. These deformations are caused by removing and interpolating the metal projection rays. This leads to information loss, especially about the edges crossing the removed projection rays.

The iterative methods use all available information and should give better reconstruction of the metal surrounding. Artefact reduction is achieved by the use of a more sophisticated reconstruction model. The additional computation time is limited in this study by applying this sophisticated model locally, in the metal regions, and keeping the model more simple for the remainder. The local model reconstruction proposed in this work can assign a different energy and resolution model to particular parts of the reconstruction volume. As can be seen in figure 1 and 2, a regular *IMPACT* reconstruction still results in an image with clear streaks in between the metals. These artefacts are reduced in the *Patched IMPACT* reconstruction. One could attribute this to the different resolution model but this is not the main reason. In figure 3, a reconstruction with and without increased resolution is shown for the body phantom. In both cases a sequential update was used for the different patches. This result shows that the substantial artefact reduction comparing *IMPACT* with *Patched IMPACT* is not due to the resolution modelling but due to the updating scheme.

Sequential updates of pixel groups is known to improve the convergence [9]. The smaller the group the bigger the update. Thus, smaller patches get a bigger update. The separate update of the patches changes the relative convergence of the metals compared to the rest of the image, resulting in better attenuation values and sharper edges for the metals and fewer artefacts.

The full local model reconstruction can also change the energy model of each of the patches. The IMPACT model was used for all metals, MLTRC for the remainder of the reconstruction volume. For both phantoms, a very similar image quality is obtained when using MLTRC instead of IMPACT. When considering the (back)projections as a measure for computational complexity (and time), we obtain a reduction from 8 to 3 (back)projections.

The reconstructions with *Patched IMPACT* and *MLTRC+IMPACT* still have some remaining artefacts. They could possibly be reduced by using a more accurate model for the metals. However, the artefact reduction achieved when comparing *IMPACT* with *Patched IMPACT*, suggests that the model is possibly not the main factor. *IMPACT* and *Patched IMPACT* (without resolution modelling) use the same model but result in a different image just by changing the relative convergence of the image parts. This suggests that the optimum for the likelihood is flat and different solutions can be achieved when using a finite iteration number. The use of priors can be a solution to guide the algorithm to the desired reconstruction. Note that also here the properties of the prior could be changed depending on the particular patch.

VI. Conclusion

PC methods are fast and efficient methods for metal artefact reduction but they tend to deform structures lying in the interpolated projection rays. Iterative methods result often in more pronounced shadow and streak artefacts but yield a better reconstruction of structures around and in between metals. The increased computation time caused by the more complex model can be limited by applying the more sophisticated model only locally in and around the metals. This local model reconstruction does not result in loss of image quality. Moreover, the sequential nature of updating the different image parts leads to an improved artefact reduction.

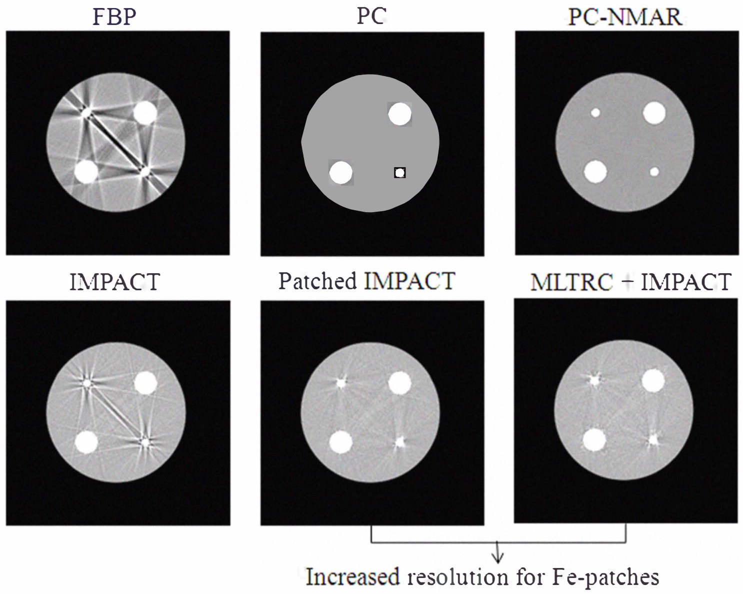

Fig. 1. **Circular phantom**. Top row: reconstruction with FBP, PC and PC-NMAR, bottom row: regular IMPACT reconstruction, patched IMPACT with increased resolution for the patches containing iron and full local model reconstruction with IMPACT for metal patches and MLTRC for non-metal patches. Windowed in interval [-700, 500] HU.

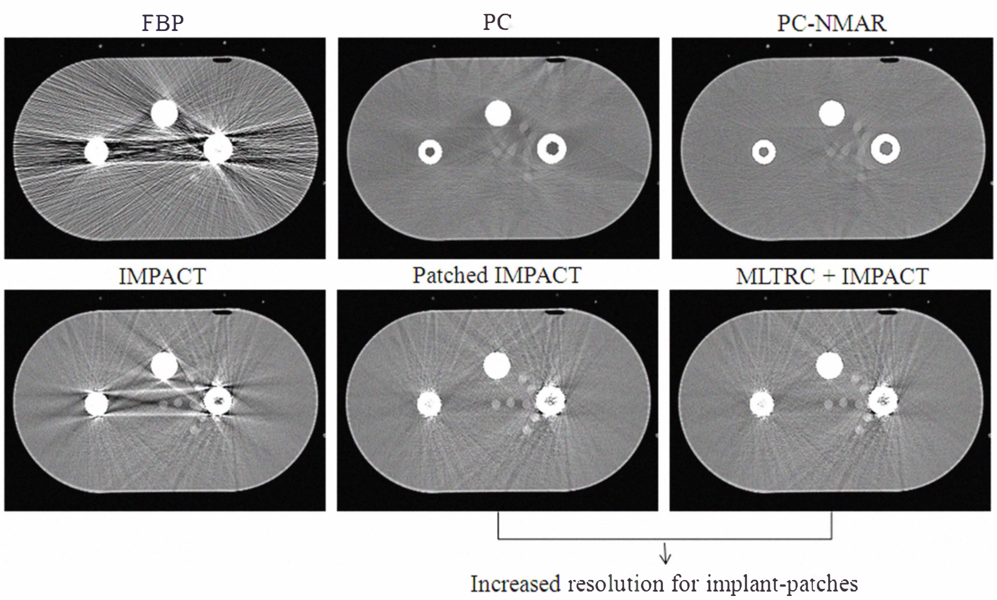

Fig. 2. **Body shaped phantom**. Top row: reconstruction with FBP, PC and PC-NMAR, bottom row: regular IMPACT reconstruction, patched IMPACT with increased resolution for the patches containing implants and full local model reconstruction with IMPACT for metal patches and MLTRC for non-metal patches. Windowed in interval [-700, 500] HU.

VII. Acknowledgement

The authors would like to thank Karl Stierstorfer from Siemens Healthcare Sector, Germany for his valuable suggestions and help with the data format.

References

[1] Kalender W. et al. “Reduction of CT artifacts caused by metallic impants.” *Radiology*, 1987; 164: 567-568. *Phys. Med. Biol.*, 2004; 49:145-157.

[2] Glover G. and Pelc N. “An algorithm for the reduction of metal clip artifacts in CT reconstructions.” *Med. Phys.*, 1981; 8 (6): 799-807.

[3] Mahnken A. et al, “A new algorithm for metal artifact reduction in computed tomogrpahy, In vitro and in vivo evaluation after total hio replacement.” *Investigative Radiology*, 2003; 38 (12): 769-775.

[4] Barrett J. F. and Keat N., “Artifacts in CT: Recognition and avoidance.”, *RadioGraphics*, 2004; 24:1679-1691.

[5] De Man B. et al, “Metal streak artifacts in X-ray computed tomography: a simulation study.” *Trans. Nucl. Sci.*, 1999; 46 (3):691-696.

[6] Van Slambrouck K. and Nuyts J, “A patchwork (back)projector to accelerate artifact reduction in CT reconstruction.” IEEE Nucl Sci Symp Conf Record, Knoxville, TN, USA, oct-nov 2010.

[7] Nuyts J. et al, “Iterative reconstruction for helical CT: a simulation study.” *Phys. Med. Biol.*, 1998; 43: 729-737.

[8] De Man B. et al, “Iterative maximum-likelihood polychomatic algorithm for CT.” *Trans. Med. Im.*, 1995; 14 (1):132-137.

[9] Fessler J.A. et al, "Grouped-coordinate ascent algorithm for penalized-likelihood transmission image reconstruction." *Trans. Med. Im.*, 1997; 16 (2): 166-175.
[10] De Man B. and Basu S., "Distance-driven projection and backprojection in three dimensions." *Phys. Med. Biol.*, 2004; 49: 2463-2475.
[11] Muller J., Buzug T.M., "Spurious structures created by interpolation-based Ct metal artifact reduction." *Proc. of SPIE*, 2009; 7258: 72581Y1 - 72581Y8.
[12] Meyer E. et al, "Normalized metal artifact reduction (NMAR) in computed tomography." *Med. Phys.*, 2010; 37 (10): 5462-5493